Study of Structural, Dielectric, and Phase Transition of Strontium Doped $BaTiO_3$

Asmaa Zouitine[1], Abdelhak El Ghandouri[2], Abdelhalim Elbasset[2,3*], Farid Abdi[3], Taj-dine Lamcharfi[3], Hicham Laribou[4], Lamiae Mrharrab[2], and Zouhairi Mohammed[5]

[1]*Laboratory of Instrumentation of Measure and Control (LIMC), Department of Physics, Faculty of Sciences, University Chouaib Doukali, El Jadida 24000, Morocco*

[2]*LPAIS, Faculty of Science Dhar El Mahraz, Sidi Mohamed Ben Abdellah University of Fez, Fez 30050, Morocco*

[3]*Signals, Systems and Components Laboratory (LSSC), Faculty of Sciences and Technologies of Fez, Sidi Mohamed Ben Abdellah University, Fez 30050, Morocco*

[4]*Laboratory for Microstructures and Materials Mechanics, University of Lorraine, Metz 57070, France*

[5]*Team of Materials, Membranes and Separation Processes, Faculty of Sciences, Moulay Ismail University of Meknes, Meknes 50060, Morocco*

* ***Corresponding author:***

email: abdelhalim.elbasset@usmba.ac.ma

Received: January 29, 2024
Accepted: October 15, 2024

DOI: 10.22146/ijc.93659

Abstract: *In this paper, we studied the effect of strontium doping on the structural, microstructural, dielectric, and electrical properties of $Ba_{1-x}Sr_xTiO_3$ (BS_xT) ceramics prepared via the sol-gel method, with x = 0.00 to 0.15. The results obtained from the X-ray diffraction spectrum confirmed the creation of the pure perovskite structure, with the diffraction peaks of the BS_xT shifting toward the bigger 2θ with increasing Sr content. Scanning electron microscopy images show that the grain size of the BS_xT ceramics decreases with increasing Sr content. An increase in Sr content appears to lower the activation energy by the factor of 0.16 meV/mol% and to decrease Curie temperature by the factor of 3.34 °C/mol%. Furthermore, in case of 15 mol% of Sr addition, the dielectric constant value is increased about twice. Moreover, the relationship between grain sizes and dielectric properties was also investigated. Using the frequency measurement method (up to 2 MHz in a step of 1 kHz), we are able to determine the temperature of transition without using the conventional method.*

Keywords: *$Ba_{1-x}Sr_xTiO_3$; frequency of relaxation; phase transition; activation energy; dielectric properties*

■ INTRODUCTION

Ferroelectric materials of the ABO_3 type perovskite crystal structure have been widely used in microelectronic industries due to their high dielectric constant and low leakage current [1-4]. The most important examples of ferroelectric materials are $BaTiO_3$ and $SrTiO_3$. $BaTiO_3$ is ferroelectric, and the origin of ferroelectricity is derived from the displacement of ions relative to each other. This compound has been used for a long time in various industrial sectors. One of these sectors, currently on the rise, is that of multilayer ceramic capacitors [5-6]. An exciting and highly contemporary application of $BaTiO_3$ involves the development of ferroelectric random-access memories for computers [7]. Its optical and electrical properties have proven to be technologically promising for linear resonators, sensors, actuators, laser phase matching, spatial light modulators, optical waveguides, energy-storage components, and high-frequency filters [6,8-11].

It is also well known that specific properties of $BaTiO_3$ can be systematically changed by the chemical substitution of barium and/or titanium by a wide variety of isovalent and aliovalent dopants [6,10-11]. For example, doping of $BaTiO_3$ with strontium ($Ba_{1-x}Sr_xTiO_3$ or BS_xT) has been a vital material [12-15] for tunable microwave devices such as phase shifters, tunable filters, delay lines, tunable oscillators, and induced piezoelectric

transducer. This is because of its high dielectric constant, sizeable electric field turnability, relatively low dielectric loss, variable Curie temperature (from −243 to 127 °C) depending on the composition of strontium, large polarizations, large permittivity, and large induced strains that are achievable. On the other hand, it is known that the temperature and the frequency in perovskite structure-type materials influence all the properties mentioned above. Therefore, the temperature dependence of the dielectric permittivity for some frequencies has been widely studied and reported as an essential feature to determine the temperatures and character of the phase transition in ferroelectric materials [16-18].

To the best of our knowledge, no work focusing on the study of the dielectric properties in the BS_xT system in an extensive frequency interval and for different temperatures of measure has been reported in the literature, except that which is narrated by Mahani et al. [19] but only for few frequencies. Therefore, in the present work, a detailed investigation was performed concerning the evolution of the dielectric constant according to the frequency for different temperatures of measure. Indeed, to determine the transition temperature, we have found a different approach than the method used in previous studies. Therefore, the objective of this study is to synthesize BS_xT ceramics with x = 0.0, 2.5, 5.0 7.5, 10, 12.5, and 15 mol% through the sol-gel method to investigate the effect of the Sr^{2+} cations on the structural, microstructural, dielectric and electrical properties of these materials.

■ EXPERIMENTAL SECTION

Materials

In this study, we utilized high-purity barium acetate ($Ba(CH_3CO_2)_2{\cdot}3H_2O$ (99.9%, Johnson Matthey GmbH Alfa, Karlsrube, Germany), strontium carbonate ($SrCO_3$), and titanium alcoxide ($Ti[O(CH_2)_3CH_3]_4$, 97%, Johnson Matthey GmbH Alfa, Karlsrube, Germany).

Instrumentation

The crystallinity and phases of the powders were examined using X-ray diffraction (XRD). The microstructure of the powders was characterized by scanning electron microscopy (SEM) with a JEOLJS M6390 associated with a 0.530 kV adjustable Bruker source. Computer-assisted dielectric characterization was performed as a function of the frequency from 1 kHz up to 2 MHz using an LCR meter (HP Model 4284A), which covers a frequency range of 20 Hz to 2 MHz. These dielectric measurements were carried out in the 30–225 °C temperature range and sub-weak level of excitement.

Procedure

Pure $BaTiO_3$ and BS_xT (where x = 0.0, 2.5, 5.0 7.5, 10, 12.5 and 15 mol%) were prepared using the sol-gel method. In this work, stoichiometric proportions of high purity $Ba(CH_3CO_2)_2{\cdot}3H_2O$, $SrCO_3$, and $Ti[O(CH_2)_3CH_3]_4$ were used to prepare the BS_xT ceramics samples. All these antecedents were mixed thoroughly in a woodshed at 60 °C while being constantly stirred.

The nominal amounts of $Ba(CH_3COO)_2{\cdot}3H_2O$ and $SrCO_3$ powders were first dissolved in water and acetic acid and stirred at 60 °C until the solution became transparent and cooled down to room temperature. The $Ti[O(CH_2)_3CH_3]_4$ solution was added in citric acid by stirring at 50–60 °C. After the above solution turned clear, the BS_xT solution was prepared by mixing both solutions stoichiometrically. The resulting solution became transparent sols at 50–60 °C and then formed gels at 80 °C for 140 h. A detailed explanation of the remaining steps in preparing for BT and BS_xT is provided in another work [20]. This xerogel was finely ground in an agate mortar to obtain a homogeneous powder. This powder was then calcined in air at 900 °C for 4 h, cooled to room temperature, and milled again. These compositions were then mixed with polyvinyl alcohol as a binder. They were pressed into pellets of 12 mm in diameter and thickness of 1 mm using a press with a uniaxial pressure equal to 10 h/cm^2. The pelletized samples were sintered at 1100 °C for 8 h in a programmable furnace. The silver paste was added to both faces of the disks, which were then fired at 60 °C as electrodes.

■ RESULTS AND DISCUSSION

XRD patterns of the BS_xT with various Sr content were shown in Fig. 1(a). Fig. 1(b) is an enlarged picture with a 2θ range of 44–45°. It indicates that the increase

in the doping rate by Sr causes a shift in the position of the peak (002/200) towards the largest angles, highlighting incorporation and the effect of Sr on $BaTiO_3$. The decrease in grain size can explain the increasing width peak with the increase in doping because the materials with larger crystal sizes have a sharp diffraction pattern, while materials with smaller ones experience peak widening [21].

Fig. 2 shows microstructures of BS_xT ceramics sintered at 1100 °C for 8 h. The grain size was determined by averaging each micrograph's total number of grain sizes. The obtained BS_xT ceramic was homogeneous. The grain size decreased from over 1.75 to 0.56 μm with Sr concentration from 0 to 0.15 mol%. Porosity was observed and decreased over the 0.15 mol% of Sr concentration. Therefore, the bulk density was increased (Fig. 3) due to reduced porosity. It is clear from the micrographs that a highly dense microstructure can be obtained together with decreasing grain size by increasing the value of x, which may be due to the Sr ions segregation at the grain boundaries, thus inhibiting grain growth.

Fig. 4 shows the variation of the dielectric constant, ε_r, as a function of frequency at different temperatures for all the samples. For pure $BaTiO_3$, to a given temperature, the curve of ε_r presents a particular evolution as a function of frequency. Indeed, when the frequency increases, ε_r passes through a maximum, decreases, passes through a minimum, and increases after that. It is a phenomenon identical to a relaxation at a given frequency. Therefore, the trend of variation of ε_r with frequency is typical of the presence of electrical relaxation phenomena, which is

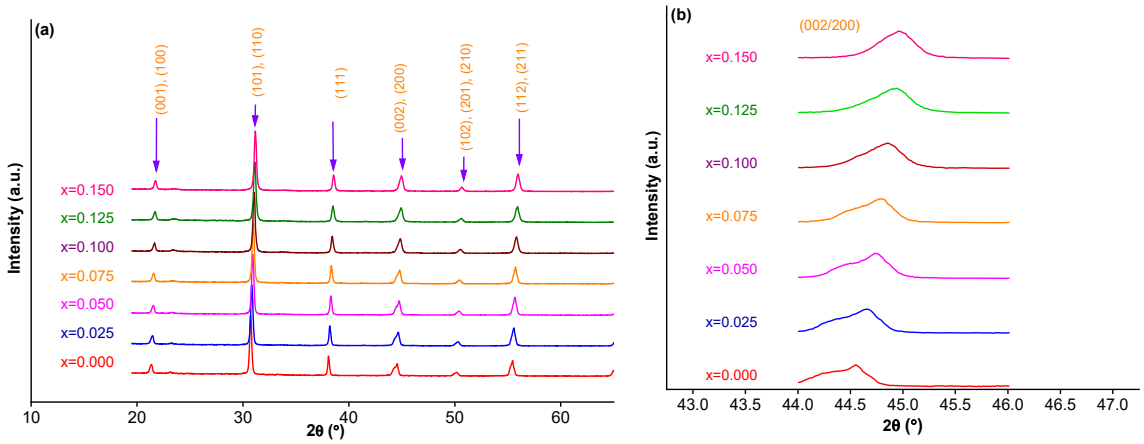

Fig 1. XRD patterns of (a) the BS_xT with various Sr content and (b) shift of (002/200) diffraction peak of BS_xT to superior diffraction angle with the increase in Sr content

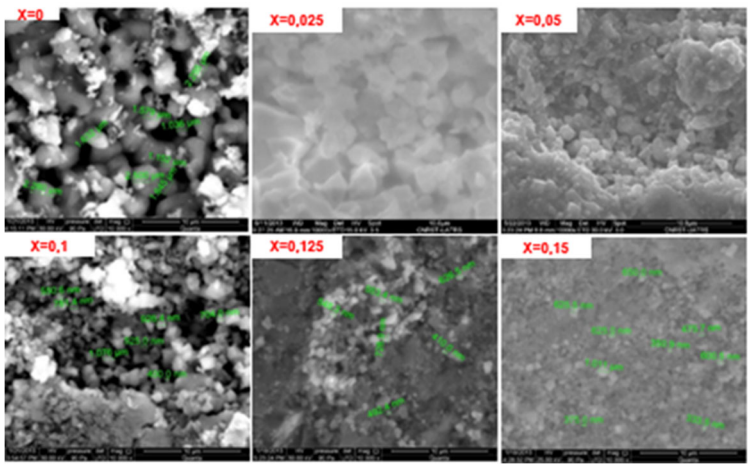

Fig 2. SEM micrographs of polished and thermally etched surface of BS_xT specimens sintered at 1100 °C

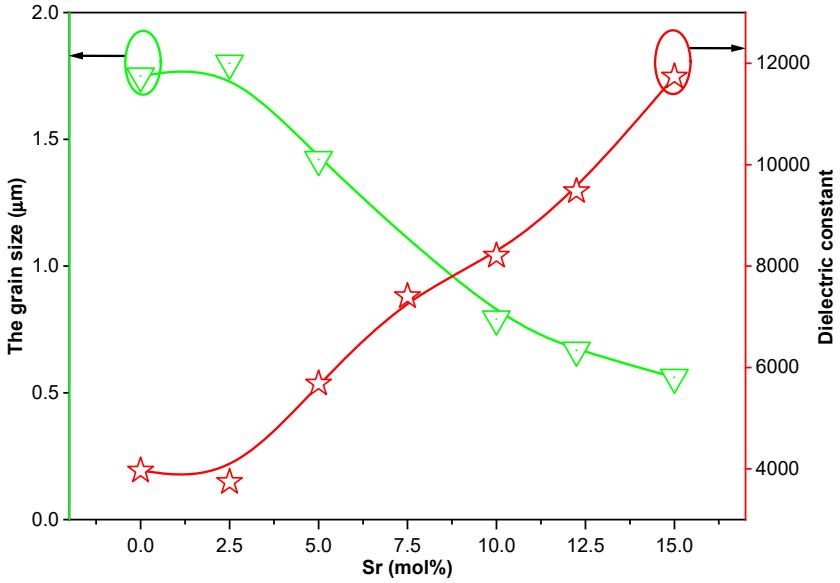

Fig 3. Variation of maximum dielectric constants and the grain size as a function of Sr contents in BS_xT

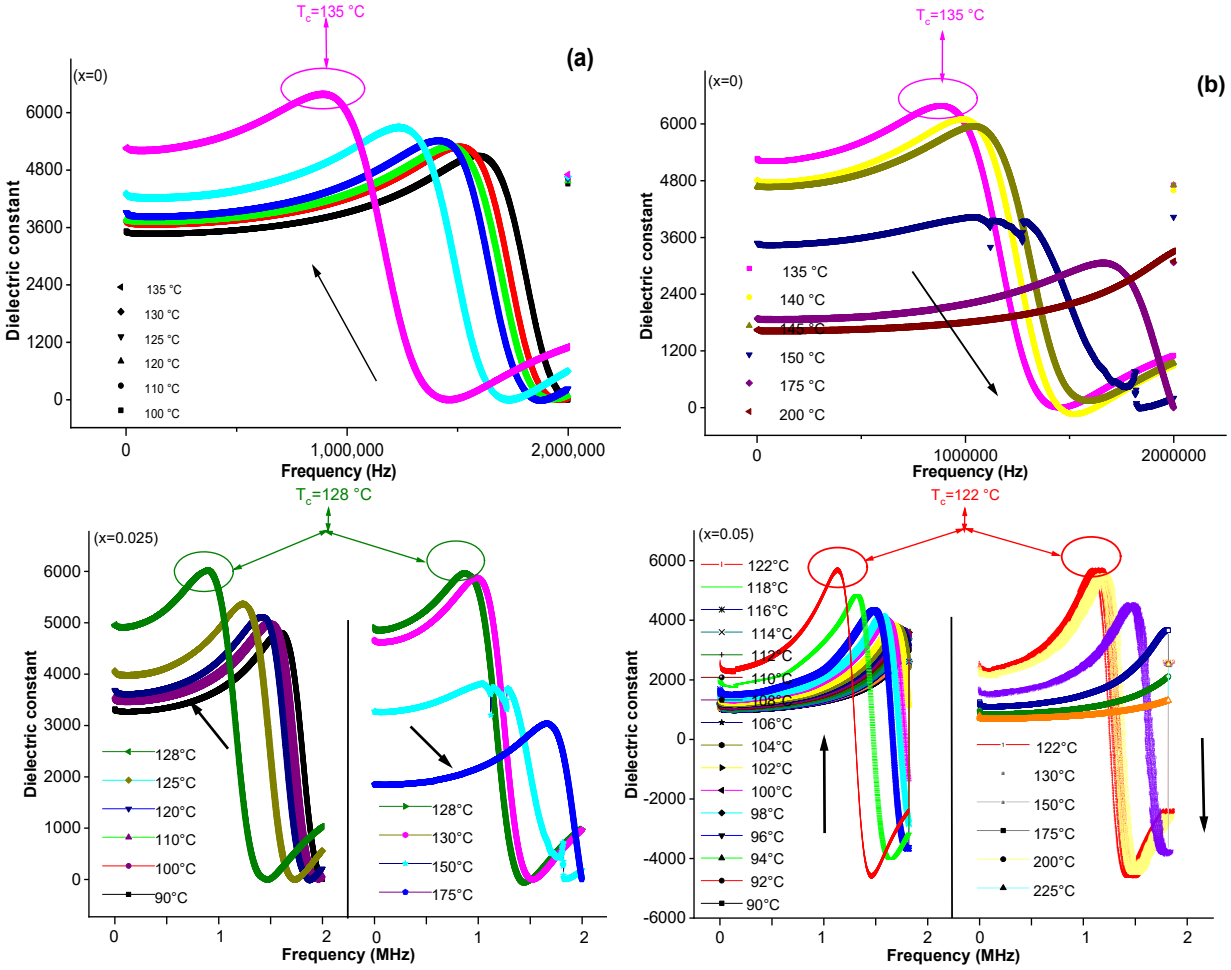

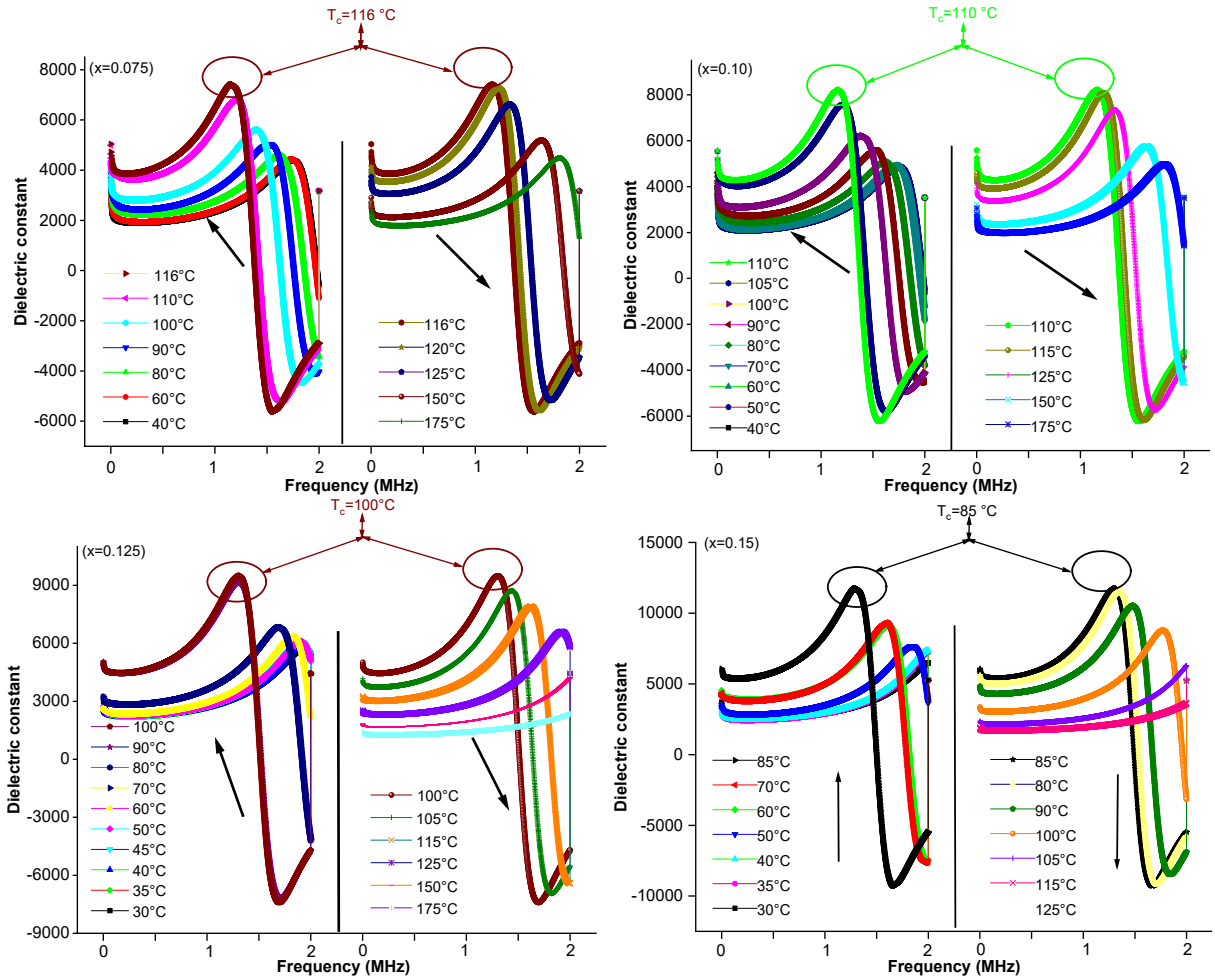

Fig 4. Frequency-dependent dielectric constant of BS_xT at (a) all temperatures below 135 °C and (b) all temperatures higher than 135 °C

temperature-dependent. The ε_{rmax} for pure $BaTiO_3$ moves when the temperature changes. Furthermore, for all temperatures below 135 °C (Fig. 4(a)), this shift is carried out towards lower frequencies when the temperature of measurement increases. However, this tendency is inverted for temperatures higher than 135 °C (Fig. 4(b)). Fig. 5(a) illustrates the evolution of this frequency of relaxation according to the temperature for pure $BaTiO_3$. It demonstrates that the frequency associated with ε_{rmax} decreased to a minimum value (f_m = 880 kHz) at T = 135 °C, and then increased for higher temperatures. According to the literature, this temperature (135 °C), corresponds to the transition temperature, T_c [16-19], in which $BaTiO_3$ transits from the ferro-paraelectric phase. Therefore, the temperature has an effect of the frequency position of the dielectric relaxation towards lower frequencies in the ferroelectric phase and towards the high frequencies in the paraelectric phase. This observation is also valid for the other compounds at different concentrations Sr. On the other hand, the result found by Mahani et al. [19] indicated that the dielectric constant varies randomly with the temperature of the measure, which prevents the exact determination of T_c; this evolution is due to the destabilization of the measured temperature. For a given frequency, the dielectric constant should increase with temperature in the ferroelectric phase and decrease in the paraelectric one.

In addition, the absence of the relaxation in the work of Mahani et al. [19] is due to the fact that the values

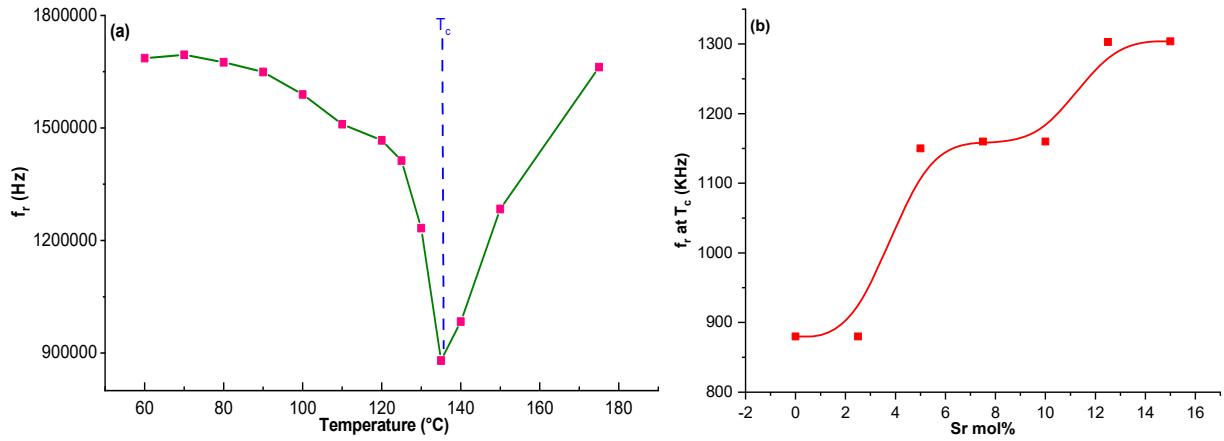

Fig 5. The evolution of the frequency of relaxation according to (a) the temperature of $BaTiO_3$ and (b) Sr mol% of BS_xT

of frequency considered are insufficient (not exceeding 46 values), especially for $BS_{10}T$ (f_r = 1.2 MHz in this case) in which the relaxation frequency is greater than 1 MHz and this relaxation occurs in the evolution of dielectric losses for few temperatures. Our result using the frequency measurement method (up 2 MHz by 1 kHz), which has never been reported in the literature, allowed us to determine the transition temperature without using other conventional methods, which consist of the temperature measurements for some frequencies and could not bring up specific effects or phenomena. The relaxation mechanism in the $BaTiO_3$ is based on the fact that the Ti^{4+} ion moves outside the center of the octahedron of oxygen and can occupy various wells of potential; the process of relaxation is associated with cooperative jumps of Ti^{4+} ions between these multiple wells. This movement would be coherent over a length, I_c, corresponding to a correlation chain.

Whatever is the composition, the frequency of the relaxation always presents a minimum near T_c (Fig. 5(a)). This minimum can be explained by the increasing number of Ti^{4+} ions, which contribute to the cooperative movement along the chains of correlation when the temperature decreases towards T_c. So, the inertia of the chain increases, and the frequency of relaxation decreases until a minimal value in the neighborhood of the temperature of transition. On the other hand, this relaxation frequency (f_r) at T_c increases when x increases from 0 to 0.15 (Fig. 5(b)). This is explained by the substitution of Sr in $BaTiO_3$, which results in a deformation of the BaO_6 octahedron, which probably implies a shorter correlation chain leading to an increase in the relaxation frequency.

This relaxation depends on the temperature and the molar fraction Ba/Sr, which is attenuated when the temperature increases. On the other hand, the amplitude of the maximum dielectric constant in the ferroelectric phase increases with the temperature, while in the paraelectric phase, it decreases when the temperature increases. In the paraelectric phase, the peaks' diminution and asymmetric broadening suggest the presence of electrical processes in the materials with a spread of relaxation time [22]. The shifting of peaks indicates that the net relaxation time is decreasing with the increase in temperature. The dielectric data was used to evaluate the relaxation time (τ) of the electrical phenomena in the material using Eq. (1);

$$\tau = \frac{1}{w_{max}} = \frac{1}{2\pi f_{max}} \quad (1)$$

where f_{max} is the relaxation frequency. The nature of the variation of τ with temperature of all the compounds is shown in Fig. 6. The curves appear to follow the Arrhenius relation, which is given in Eq. (2);

$$\tau = \tau_0 \exp\left(\frac{E_r}{kT}\right) \quad (2)$$

where τ_0 is a pre-exponential factor, E_τ is the activation energy, k is the Boltzmann constant, and T is the absolute temperature. Activation energy values evaluated from the slope of log (τ) against the 1000/T curve are 3.18, 1.51, 1.14, 0.81 meV for x = 0, 0.05, 0.10,

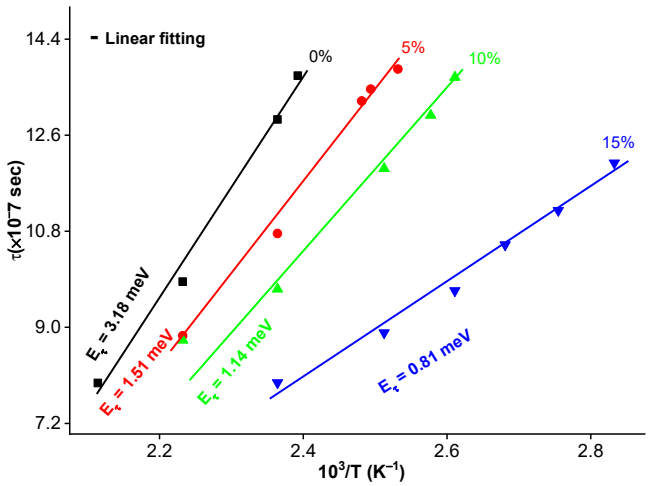

Fig 6. Variation of relaxation time with inverse of temperature of BS_xT

and 0.15, respectively. The value of activation energy decreases with an increase in Sr concentration.

The small value of activation energy may be due to the ionized oxygen vacancies. The evolution of T_c of BS_xT shows that the transition temperature varies from 135 °C for $BaTiO_3$ to 110 °C for $Ba_{0.9}Sr_{0.1}Tio_3$ (Fig. 4), and reaches a value of 85 °C for the sample doped with 15% Sr. In other words, T_c decreases by a constant factor of 6.25 °C per 2.5% by Sr up to 10% and decreases by 10 °C per 2.5% for the sample $Ba_{0.875}Sr_{0.125}TiO_3$. Therefore, the decrease in T_c becomes more significant from doping with 10% in Sr. This variation in the Curie temperature represents a modification behavior of the ferroelectric phase. An interdiffusion of atoms between the Sr and Ba sublattices can explain this phenomenon. The insertion of Sr (atomic radius Sr^{2+} = 1.14 Å) in the BT sublattice can deform the latter. A modification of the chemical bonds involves a lowering of T_c. But this reduction is more important as the proportion of Sr is large. Indeed, the atomic interdiffusion responsible for the reduction in T_c can modify the chemical composition of the ferroelectric grains. For small grains (≤ 1μm) of BS_xT (x > 10%), the diffusion of Sr^{2+} can reach the center of the grains of BS_xT. One obtains a ceramic with relatively small grains of BS_xT composition at lower T_c (see the case of x = 15%), while for powders with x < 10% in strontium, the diffusion of Sr^{2+} cannot reach the center of the coarse grains (≥ 1 μm).

Many researchers have studied the effects of grain size on dielectric properties in $BaTiO_3$ ceramics [23]. In general, ε_r is increased when the grain size is near 1 μm at room temperature, and when the grain size is larger than 1 μm, ε_r shows a slight decrease with increasing grain size. According to the domain wall model [22], the phenomenon has been explained. From the grain size point of view, the dielectric constants should decrease with increased Sr amount from the above analysis, which contradicts our results for x > 10% (Fig. 3), so it can be concluded that Sr doping significantly affects the dielectric constants in BS_xT (x > 10%) ceramics.

The curves in Fig. 7 show the variation of the dissipation factor as a function of frequency for all the samples at different temperatures. For pure $BaTiO_3$, the dielectric losses are constant and almost negligible at low frequencies (f < 1 MHz) and a given temperature. They increase rapidly with increasing frequency until reaching a maximum value, then decrease rapidly and become practically constant. The value of this maximum increases with the temperature for $T < T_m$. On the other hand, its value decreases with the temperature for $T > T_m$ (in the paraelectric phase). The increase in dielectric losses may be due to low-frequency relaxation or a diffusion phenomenon.

In the ferroelectric phase, the maximum dielectric losses move towards lower frequencies. Meanwhile, there is an opposite evolution in the paraelectric domain ($T > T_m$). This particular behavior is also observed for the other BS_xT samples. It is interesting to note that the temperature of the maximum loss as a function of frequency is similar to that of the dielectric permittivity as a function of frequency (Fig. 4). So, we can present the loss peaks as being at the origin of the variations of the permittivity according to the frequency. And as the Kramers-Kronig law states, all-dielectric losses induce variations in permittivity as a function of frequency. For this reason, when we measure any dielectric constant at a frequency, we will obtain a non-zero value of tan(δ) even if no relaxation peak is at the origin [24]. On the other hand, we note that the dielectric loss clears with the doping rate, where the values of the samples BS_xT (x = 0, 2.5, 5, 7.5, 10, and 15 mol%) at 100 °C (for f = 1 MHz) are 0.052, 0.043 and 0.029, 0.017, 0.011, 0.009, respectively.

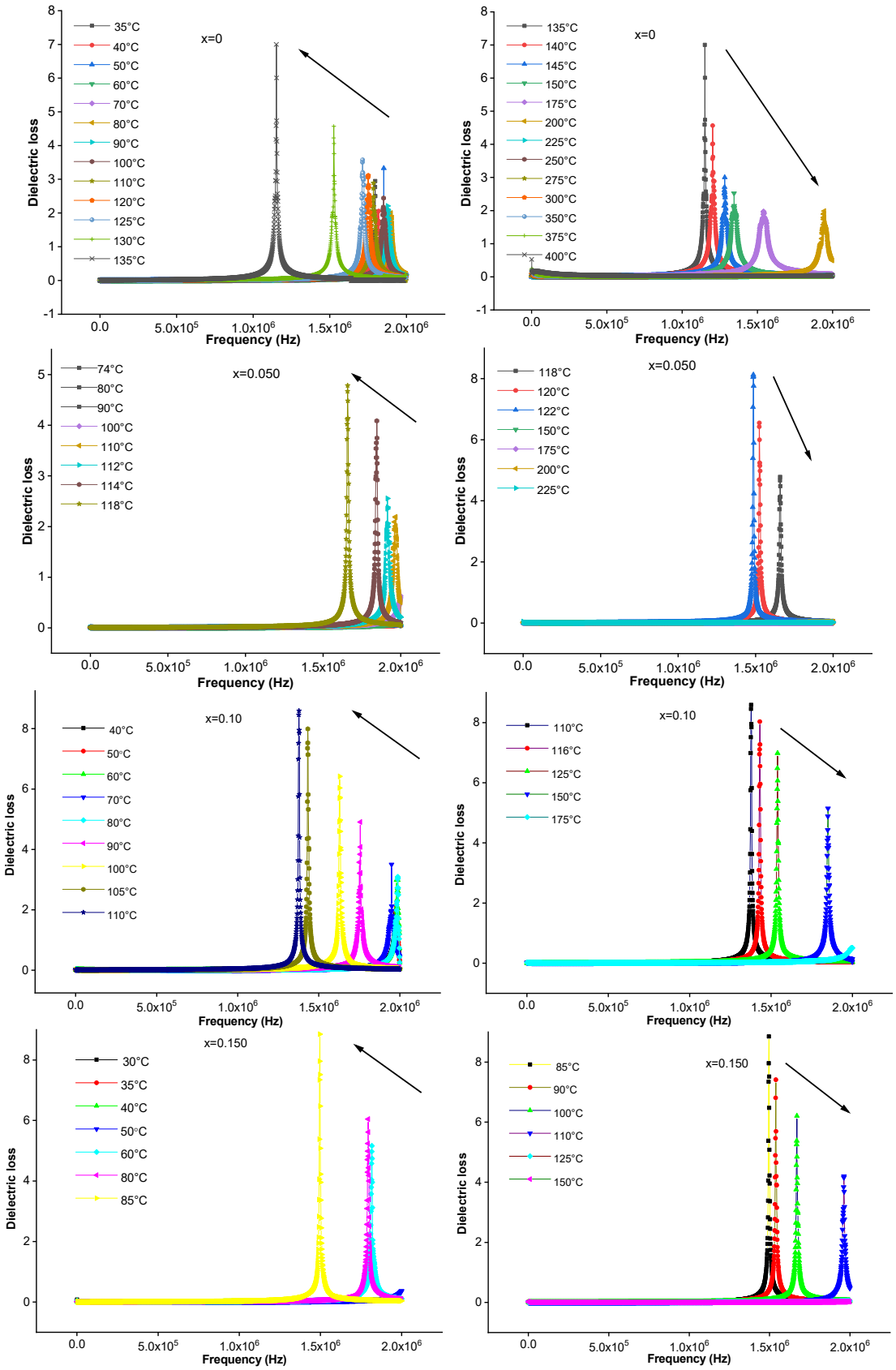

Fig 7. Frequency dependent dielectric loss (tan δ) of BS_sT system containing various amounts of Sr

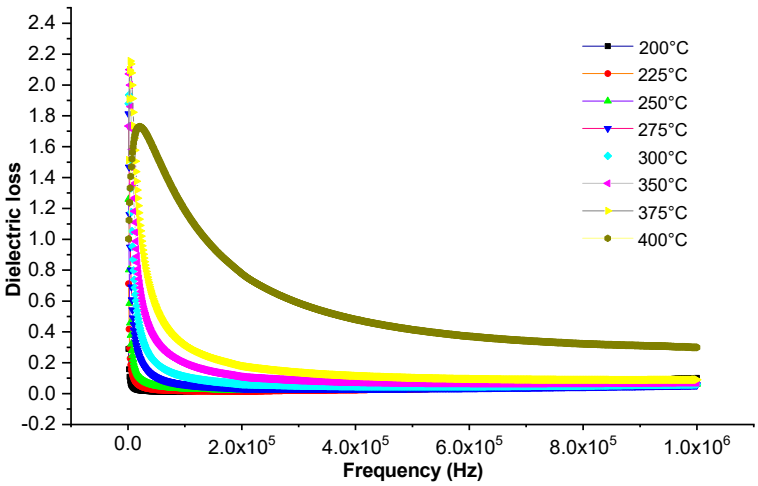

Fig 8. Frequency dependences of dielectric loss (tan δ) nanocrystalline ceramic $BaTiO_3$ at various temperatures

These values are very small in comparison with other work [16]. Therefore, after all that we have just seen, we can deduce that the samples BS_xT have more minor and stable dielectric losses as a function of frequency, which provide a large scale of several application fields such as surge protection of electronic devices. Finally, the dielectric study shows higher responses at lower optimal operating temperatures compared to other work [25-26].

The curves of the dielectric losses of $BaTiO_3$ as a function of the frequency in the temperature interval of 200–400 °C (Fig. 8), show that the values of the dissipation factor decrease as the frequency increases. This characterizes a normal behavior for ferroelectrics [27]. At sufficiently low frequencies, all the moments reorient themselves in the direction of the field, and all the polarization mechanisms are involved. Polarization is then maximum implies a phase shift that can occur between the tilting of the field and the reorientation of the dipole moments; this phenomenon is at the origin of the dissipation of part of the energy of the field in the material around a so-called relaxation frequency f_r [28].

■ CONCLUSION

The XRD results demonstrate that the BS_xT ceramics (where x = 0.00 to 0.15) were prepared using the sol-gel method and crystallized in the perovskite phase without secondary phases. SEM shows that the grain size of the BST ceramics decreases with increasing Sr content, which favors the decrease of T_c and the dielectric constant increase Furthermore, the value of activation energy is decreased about four times with increasing of Sr content. Significantly, we note that the dielectric loss clears with the doping rate, where the values of the samples BS_xT (x = 0, 2.5, 5, 7.5, 10 and 15 %) at 100 °C (for f = 1 MHz) are 0.052, 0.043, 0.029, 0.017, 0.011, and 0.009, respectively. These values are very small in comparison with other work. Therefore, we can deduce that the samples BS_xT have a smaller and stable dielectric loss as a function of frequency (f < 1 MHz), which provides a large scale of several application fields such as surge protection of electronic devices.

■ ACKNOWLEDGMENTS

The authors express their sincere gratitude for the assistance and support received from the Innovation Centre of the University of Fez in processing the samples for this research.

■ CONFLICT OF INTEREST

The authors declare that they have no known competing financial interests or personal relationships that could have appeared to influence the work reported in this paper.

■ AUTHOR CONTRIBUTIONS

Abdelhalim Elbasset, Farid Abdi, Taj-dine Lamcharfi, and Lamiae Mrharrab conducted the experiment and dielectric measurements. Asmaa Zouitine, Abdelhak El Ghandouri, and Abdelhalim Elbasset conducted the DRX and SEM micrographs.

Asmaa Zouitine, Abdelhalim Elbasset, and Zouhairi Mohammed wrote and revised the manuscript. All authors agreed to the final version of this manuscript.

■ REFERENCES

[1] Kumawat, N., and Jindal, S., 2023, Comparative study of structural and dielectric property of rare earth metal and transition elements doped tungsten bronze, *Mater. Today: Proc.*, 2023, In Press, Corrected Proof.

[2] Wang, Y., Cao, X., Zhang, J., Lin, H., and Wang, Z., 2023, Nb^{5+}-doped $SrTiO_3$-based glass-ceramics: Insight into crystallisation kinetics, microstructure, and dielectric properties, *Ceram. Int.*, 49 (11, Part A), 17415–17423.

[3] Zheng, M., Guan, P., Yang, J., and Zhang, Y., 2023, Microstructure and composition driven ferroelectric properties of Er^{3+} doped lead-free multifunctional $0.94Bi_{0.5}Na_{0.5}TiO_3$-$0.06BaTiO_3$ ceramics, *Ceram. Int.*, 49 (18), 30481–30489.

[4] Mesrar, M., Elbasset, A., Echatoui, N.S., Abdi, F., and Lamcharfi, T., 2023, Microstructural and high-temperature dielectric, piezoelectric and complex impedance spectroscopic properties of $K_{0.5}Bi_{0.5}TiO_3$ modified NBT-BT lead-free ferroelectric ceramics, *Heliyon*, 9 (4), e14761.

[5] Reavley, M.J.H., Guo, H., Yuan, J., Ng, A.Y.R., Ho, T.Y.K., Tan, H.T., Du, Z., and Gan, C.L., 2022, Ultrafast high-temperature sintering of barium titanate ceramics with colossal dielectric constants, *J. Eur. Ceram. Soc.*, 42 (12), 4934–4943.

[6] Yadav, A.K., Fan, H., Yan, B., Wang, W., Dong, W., and Wang, S., 2021, Structure evolutions with enhanced dielectric permittivity and ferroelectric properties of $Ba_{(1-x)}(La,Li)_xTiO_3$ ceramics, *J. Mater. Sci.: Mater. Electron.*, 32 (18), 23103–23115.

[7] Mikanshi, M., Chaudhary, S., Devi, S., and Jindal, S., 2023, Comparison of structural and dielectric properties of doped (M, R and A) barium strontium titanate: Review, *Mater. Today: Proc.*, 2023, In Press, Corrected Proof.

[8] Gajula, G.R., Buddiga, L.R., and Vattikunta, N., 2019, The effect of Sm and Nb on impedance spectroscopy and high frequency modulus, complex modulus, conductivity studies of $BaTiO_3$-$Li_{0.5}Fe_{2.5}O_4$ ceramics, *Mater. Chem. Phys.*, 230, 331–336.

[9] Damamme, R., Seveyrat, L., Borta-Boyon, A., Nguyen, V.C., Le, M.Q., and Cottinet, P.J., 2023, 3D printing of doped barium-titanate using robocasting - Toward new generation lead-free piezoceramic transducers, *J. Eur. Ceram. Soc.*, 43 (8), 3297–3306.

[10] Yan, G., Ma, M., Li, C., Li, Z., Zhong, X., Yang, J., Wu, F., and Chen, Z., 2021, Enhanced energy storage property and dielectric breakdown strength in Li^+ doped $BaTiO_3$ ceramics, *J. Alloys Compd.*, 857, 158021.

[11] Chchiyai, Z., El Bachraoui, F., Tamraoui, Y., Haily, E.M., Bih, L., Lahmar, A., El Marssi, M., Alami, J., and Manoun, B., 2022, Effect of cobalt doping on the crystal structure, magnetic, dielectric, electrical and optical properties of $PbTi_{1-x}Co_xO_{3-\delta}$ perovskite materials, *J. Alloys Compd.*, 927, 166979.

[12] Gong, N., and Ma, T.P., 2016, Why is FE-HfO_2 more suitable than PZT or SBT for scaled nonvolatile 1-T memory cell A retention perspective, *IEEE Electron Device Lett.*, 37 (9), 1123–1126.

[13] Dai, W., Li, Y., Jia, C., Kang, C., Li, M., and Zhang, W., 2020, High-performance ferroelectric non-volatile memory based on La-doped $BiFeO_3$ thin films, *RSC Adv.*, 10 (31), 18039–18043.

[14] Mo, F., Tagawa, Y., Jin, C., Ahn, M., Saraya, T., Hiramoto, T., and Kobayashi, M., 2020, Low-voltage operating ferroelectric FET with ultrathin IGZO channel for high-density memory application, *IEEE J. Electron Devices Soc.*, 8, 717–723.

[15] Huang, W., Zu, H., Zhang, Y., Yin, X., Ai, X., Li, J., Li, C., Li, Y., Xie, L., Liu, Y., Xiang, J., Jia, K., Li, J., and Ye, T.C., 2022, Ferroelectric vertical gate-all-around field-effect-transistors with high speed, high density, and large memory window, *IEEE Electron Device Lett.*, 43 (1), 25–28.

[16] Arshad, M., Du, H., Javed, M.S., Maqsood, A., Ashraf, I., Hussain, S., Ma, W., and Ran, H., 2020,

Fabrication, structure, and frequency-dependent electrical and dielectric properties of Sr-doped $BaTiO_3$ ceramics, *Ceram. Int.*, 46 (2), 2238–2246

[17] Ma, S., Wang, Z., Yang, L., He, D., Yang, M., Tong, L., Zhou, X., and Fan, T., 2023, Effect of Sr doping and temperature on the optical properties of $BaTiO_3$, *Ceram. Int.*, 49 (15), 26102–26109.

[18] Moussi, R., Bougoffa, A., Trabelsi, A., Dhahri, E., Graç, M.P.F., Valente, M.A., Barille, R., and Rguiti, M., 2022, Investigation of the effect of Sr-substitution on the structural, morphological, dielectric, and energy storage properties of $BaTiO_3$-based perovskite ceramics, *Inorg. Chem. Commun.*, 137, 109225.

[19] Mahani, R.M., Battisha, I.K., Aly, M., and Abou-Hamad, A.B., 2010, Structure and dielectric behavior of nano-structure ferroelectric $Ba_xSr_{1-x}TiO_3$ prepared by sol–gel method, *J. Alloys Compd.*, 508 (2), 354–358.

[20] Mesrar, M., Mesrar, L., Elbasset, A., Echatoui, N., Abdi, F., and Lamcharfi, T., 2024, Study on the structure, morphology, dielectric, and piezoelectric properties of large-grain $(Ba_{0.85}Sr_{0.15})_{1-x}Pb_xTiO_3$ ceramic system for $0.02 \leq x \leq 0.08$, *ACS Oméga*, 9 (33), 35548–35559.

[21] Ulfa, M., and Ali, M.A.P., 2022, Influence of calcination temperatures on gunningite-based gelatin template and its application as ibuprofen adsorption, *Indones. J. Chem.*, 22 (6), 1684–1692.

[22] Bharati, R., Singh, R.A., and Wanklyn, B.M., 1981, On electrical transport in $CoWO_4$ single crystals, *J. Mater. Sci.*, 16 (3), 775–779.

[23] Gargar, Z., Tachafine, A., Fasquelle, D., Zegzouti, A., Elaatmani, M., and Daoud, M., 2024, Grain size effects on dielectric properties of yttrium doped $BaTiO_3$ ceramics, *Phase Transitions*, 97 (6), 338–349.

[24] Seguin, B., Gosse, J.P., Sylvestre, A., Fouassier, A.P., and Ferrieux, J.P., 1998, Calorimetric apparatus for measurement of power losses in capacitors, *IMTC/98 Conference Proceedings. IEEE Instrumentation and Measurement Technology Conference. Where Instrumentation is Going (Cat. No.98CH36222)*, St. Paul, MN, USA, 602–607.

[25] Debnath, A., Lalwani, S.K., Singh, S., and Sunny, S., 2022, Sunny Improvement in ferroelectric properties of $BaTiO_3$ film by Mn/Sr doping for non-volatile memory applications, *Micro Nanostruct.*, 171, 207421.

[26] Tang, Q., Shi, Z., Han, M., He, Q., Dastan, D., Liu, Y., and Fan, R., 2023, Layered $SrTiO_3/BaTiO_3$ composites with significantly enhanced dielectric permittivity and low loss, *Ceram. Int.*, 49 (14, Part A), 23326–23333.

[27] He, Z., Ma, J., and Zhang, R., 2004, Investigation on the microstructure and ferroelectric properties of porous PZT ceramics, *Ceram. Int.*, 30 (7), 1353–1356.

[28] Le Paven-Thivet, C., Ishikawa, A., Ziani, A., Le Gendre, L., Yoshida, M., Kubota, J., Tessier, F., and Domen, K., 2009, Photoelectrochemical properties of crystalline perovskite lanthanum titanium oxynitride films under visible light, *J. Phys. Chem. C*, 113 (15), 6156–6162.